

Differential Dynamic Modulus of Polyisobutylene with High Molecular Weight. 2. Double-Step Large Shearing Deformations

Yoshinobu Isono,* Kouichi Shizuru, and Teruo Fujimoto

Department of Materials Science and Technology, Nagaoka University of Technology, Nagaoka, Niigata 940-21, Japan

Received September 17, 1990; Revised Manuscript Received March 11, 1991

ABSTRACT: Simultaneous measurements of stress relaxation and differential dynamic modulus were made at 20 °C for polyisobutylene with a viscosity-average molecular weight 9.6×10^5 in double-step large shearing deformations with intermittently superposed small oscillations at a frequency 0.1 Hz, which falls in the middle of the plateau zone of the polymer. The first and the second strains, γ_1 and γ_2 , were applied with an interval of time. γ_1 was constant, 2.0. γ_2 varied from 2.0 to -4.0. The experiments showed that the differential dynamic modulus never exceeded the value in the first strain by imposition of any second strain. It was concluded that the strain externally given to polymeric materials can destroy the entanglement structure but cannot recover the structure destroyed previously.

Introduction

The nonlinear viscoelastic properties of well-entangled linear polymers may be determined by the deformation of molecular chains and the change in the entanglement structure. In discussing stress relaxation after imposition of large step strains, it has been commonly assumed that not only the configuration of the polymer chains but also the entanglement structure changes in the same manner as the macroscopic deformation does.^{1,2} In a wide sense, we call this the affine assumption. Of course, nonaffine motions such as chain contraction³ have been taken into account for a short-time region at $t \sim \tau_e$, where τ_e is a characteristic time in an equilibration process.³ However, for a long-time region at t greater than a characteristic time τ_k , where the strain and time dependences of the relaxation modulus become separable, the affine assumption is widely adopted.

In the preceding paper in this issue,⁴ it was confirmed by measuring the differential dynamic modulus during stress relaxation processes in single-step large shearing deformations that the entanglement structure really changes with the strain given to the material. In this work, moreover, we test the affine assumption by similar measurements in double-step large shearing deformations.

Materials and Method

A sample, polyisobutylene L-80 (Exxon Chemicals Company), the apparatus used, a Weissenberg Rheogoniometer R-18 (Sangamo Controls Ltd.), and also the geometry of deformation were the same as in the preceding work.⁴ Double-step finite shear deformations were applied to the sample in this study; the first shear strain, γ_1 , was applied at a time $-t_1$, followed by the second strain, γ_2 , at time zero. Positive and negative signs of γ_2 mean that the direction of the second strain is the same as and opposite to that of the first strain, respectively. The time, t_1 , selected is 1200 s and 31 620 s, corresponding to the time scales τ_k (560 s for the present sample⁴), and τ_m (the maximum relaxation time), respectively. γ_1 was kept constant, 2.0, throughout the present measurements. γ_2 was varied from 2.0 to -4.0. Other experimental conditions to measure the differential dynamic modulus were the same as in the preceding study,⁴ the temperature being always 20 °C.

Results and Discussion

If we follow the BKZ constitutive equation,⁵ a shear stress, $\sigma(\gamma_1, \gamma_2; t_1, t)$, after two step shears, γ_1 and γ_2 , are

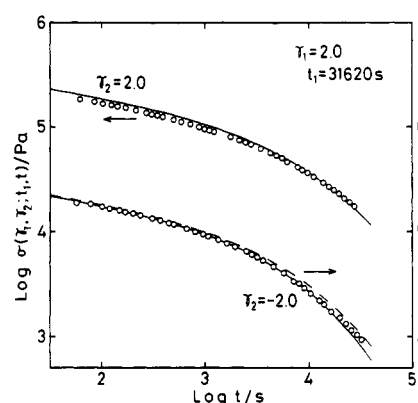


Figure 1. Double-logarithmic plots of $\sigma(\gamma_1, \gamma_2; t_1, t)$ against t for $\gamma_2 = 2.0$ and -2.0 . $t_1 = 31\,620$ s for both of the second strains. γ_1 is 2.0 throughout Figures 1-5. The solid and broken lines denote predictions of the BKZ and Doi-Edwards theories, respectively. Two theoretical curves for $\gamma_2 = 2.0$ cannot be distinguished on the graph.

applied with time interval t_1 can be expressed with a single-step relaxation of stress such as

$$\sigma(\gamma_1, \gamma_2; t_1, t) = \sigma(\gamma_2; t) + \sigma(\gamma_1 + \gamma_2; t_1 + t) - \sigma(\gamma_2; t_1 + t) \quad (1)$$

Doi proposed another equation for $\sigma(\gamma_1, \gamma_2; t_1, t)$ without use of the independent alignment approximation:⁶

$$\sigma(\gamma_1, \gamma_2; t_1, t) = \sigma(\gamma_2; t) + A(\beta)\{\sigma(\gamma_1 + \gamma_2; t_1 + t) - \sigma(\gamma_2; t_1 + t)\} - B(\alpha_2, \beta)\sigma(\gamma_2; t_1 + t) \quad (2)$$

where $A(\beta)$ and $B(\alpha_2, \beta)$ are defined in the original paper of Doi.⁶

Figure 1 shows the comparison between the data and the theories for $\sigma(\gamma_1, \gamma_2; t_1, t)$ for the cases of $\gamma_2 = 2.0$ and -2.0 at $t_1 = 31\,620$ s. Figures 2-5 show similar comparisons for various values of γ_2 at $t_1 = 1200$ s. When the stress data showed negative values, the absolute values of the stress were plotted in the figure. These were the cases for $\gamma_2 = -2, -3$, and -4 .

In the case of $t_1 = 31\,620$ s, good agreement was found between experiment and theories for both directions of γ_2 . It may be concluded that the BKZ and Doi-Edwards theories provide a fairly good description of double-step shear deformations if the time interval, t_1 , is large enough. In the case of $t_1 = 1200$ s and $\gamma_2 = 2.0, -3.0$, or -4.0 , too, agreement was found. These results agree with those

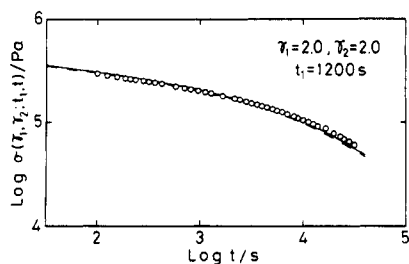


Figure 2. Double-logarithmic plots of $\sigma(\gamma_1, \gamma_2; t_1, t)$ against t for $\gamma_2 = 2.0$ and $t_1 = 1200$ s. The meanings of the lines are the same as in Figure 1.

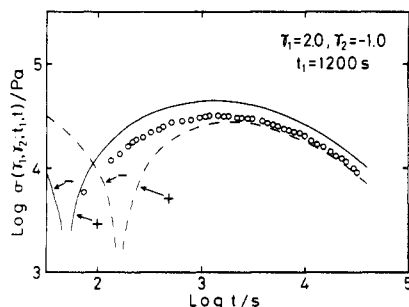


Figure 3. Double-logarithmic plots of $\sigma(\gamma_1, \gamma_2; t_1, t)$ against t for $\gamma_2 = -1.0$ and $t_1 = 1200$ s. The meanings of the lines are the same as in Figure 1. The data presented here show positive values, but theoretical predictions change the sign in the process of relaxation. The signs of the theoretical values are indicated.

reported by Osaki et al.⁷ for $\gamma_1\gamma_2 > 0$ and $\gamma_2 < -\gamma_1$. In the case of $t_1 = 1200$ s and $\gamma_2 = -1.0$ or -2.0 , however, the observed values of stress did not agree with the theoretical predictions as observed in Figures 3 and 4. It may be concluded that the utilization of the BKZ and Doi-Edwards theories gives significant errors for the double-step deformations of $-3/2\gamma_1 < \gamma_2 < 0$ if t_1 is not large. These results may imply that the second strain cannot recover the entanglement structure destroyed by the first strain. This speculation can be tested by measuring the differential dynamic modulus in double-step deformations.

Following the BKZ theory, we can calculate the differential dynamic modulus in single-step deformations and that in double-step deformations, respectively, such as

$$G'(\omega, \gamma_1; t) = \left. \frac{\partial \sigma(\gamma; t)}{\partial \gamma} \right|_{\gamma=\gamma_1} - G(0, t) + G'(\omega, 0) \quad \text{at } -t_1 < t < 0 \quad (3)$$

$$G'(\omega, \gamma_1, \gamma_2; t_1, t) = \left. \frac{\partial \sigma(\gamma; t)}{\partial \gamma} \right|_{\gamma=\gamma_2} + \left. \frac{\partial \sigma(\gamma; t_1 + t)}{\partial \gamma} \right|_{\gamma=\gamma_1+\gamma_2} - \left. \frac{\partial \sigma(\gamma; t_1 + t)}{\partial \gamma} \right|_{\gamma=\gamma_2} - G(0, t) + G'(\omega, 0) \quad \text{at } 0 < t \quad (4)$$

and

$$G''(\omega, \gamma_1; t) = G''(\omega, \gamma_1, \gamma_2; t_1, t) = G''(\omega, 0) \quad (5)$$

Figures 6–8 show the comparisons of experimental results of G' and G'' with theoretical predictions. The time interval, t_1 , was 31 620 s in Figure 6 and 1200 s in Figures 7 and 8, respectively. Experimental results and theoretical predictions are represented in the left and the right panels, respectively. The values of the differential dynamic modulus after imposition of the first and the second strains are shown by filled and open symbols, respectively. The former data (filled symbols) were in good agreement with the data of the differential dynamic modulus in a single-step deformation of $\gamma = 2.0$ in the preceding work⁴ shown by the solid lines.

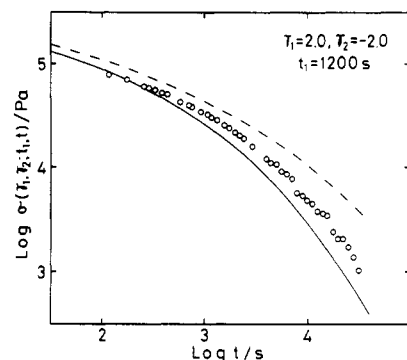


Figure 4. Double-logarithmic plots of $\sigma(\gamma_1, \gamma_2; t_1, t)$ against t for $\gamma_2 = -2.0$ and $t_1 = 1200$ s. The data and the theoretical predictions show negative values, so the absolute values of them are plotted. The meanings of the lines are the same as in Figure 1.

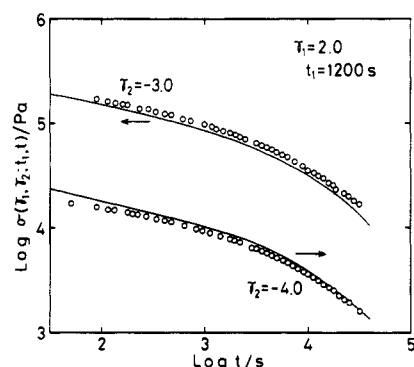


Figure 5. Double-logarithmic plots of $\sigma(\gamma_1, \gamma_2; t_1, t)$ against t for $\gamma_2 = -3.0$ (upper circles) and for $\gamma_2 = -4.0$ (lower circles). $t_1 = 1200$ s for both of the second strains. The theoretical predictions of the Doi-Edwards theory are omitted, because the BKZ and Doi-Edwards theories give almost the same and just the same values for $\gamma_2 = -3.0$ and -4.0 , respectively.

When $t_1 = 31\,620$ s, the BKZ theory predicts that the differential storage modulus after the second strain, $G'(\omega, \gamma_1, \gamma_2; t_1, t)$, is lower than that in a single-step deformation of $\gamma = 2.0$ in both directions of γ_2 . The relative position between $G'(\omega, \gamma_1; t+t_1)$ and $G'(\omega, \gamma_1, \gamma_2; t_1, t)$ was in qualitative agreement with the prediction as shown in Figure 6.

In the case of $t_1 = 1200$ s, the theory predicts that $G'(\omega, \gamma_1, \gamma_2; t_1, t)$ is lower when $\gamma_2 > 0$ or $\gamma_2 < -3/2\gamma_1$ and is higher when $-3/2\gamma_1 < \gamma_2 < 0$ than $G'(\omega, \gamma_1; t+t_1)$. In the cases of $\gamma_2 = 2.0$ and -4.0 , the values of G' in the second strain are lower than the curve for a single-step deformation of $\gamma = 2.0$ as expected.

Very interesting are the behaviors of the differential dynamic modulus in the case of $-3/2\gamma_1 \leq \gamma_2 < 0$ at $t_1 = 1200$ s (the bottom two panels in Figure 7 and the top panel in Figure 8). In these cases, the theory predicts that a recovery of G' would occur due to the second strain. However, the G' curves in the second strain are lower than or coincide with the curve in a single-step deformation of $\gamma = 2.0$. Here, the theoretical predictions of BKZ do not agree with experiments even qualitatively.

The prediction of the constancy in the differential loss modulus was not observed. The loss modulus changed in a similar way to the differential storage modulus, though the data on G'' were somewhat less precise.

In Figure 9, the values of G' at a fixed time, $t = 1000$ s, after imposition of the second strain are plotted against γ_2 . The point where γ_2 is equal to zero corresponds to that in the single-step deformation. This is shown by a chain-dashed line for comparison with the data in double-step deformations. The initial value of $G'(\omega, 0)$ measured

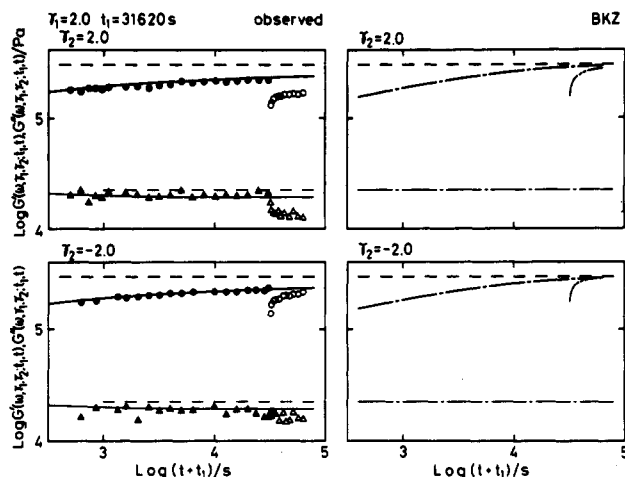


Figure 6. Logarithmic plots of differential dynamic modulus against $t + t_1$ for $\gamma_2 = 2.0$ (upper panels) and $\gamma_2 = -2.0$ (lower panels). $\gamma_1 = 2.0$ and $t_1 = 31\,620$ s. Left panels, experiments; filled circles and filled triangles denote $G'(\omega, \gamma_1; t + t_1)$ and $G''(\omega, \gamma_1; t + t_1)$, respectively; open circles and open triangles denote $G'(\omega, \gamma_1, \gamma_2; t_1, t)$ and $G''(\omega, \gamma_1, \gamma_2; t_1, t)$, respectively; the heavy and light solid lines denote the differential storage and loss modulus data for the sample L-80 in a single-step deformation of $\gamma = 2.0$ reported in the preceding paper.⁴ Right panels, predictions of the theory of BKZ; the heavy and light lines denote the values of G' and G'' , respectively; chain-dashed and chain two dashed lines denote the values in single-step and double-step deformations, respectively. In all the panels, the heavy and light broken lines denote $G'(\omega, 0)$ and $G''(\omega, 0)$, respectively. In the right panels, various light lines are overlapped.

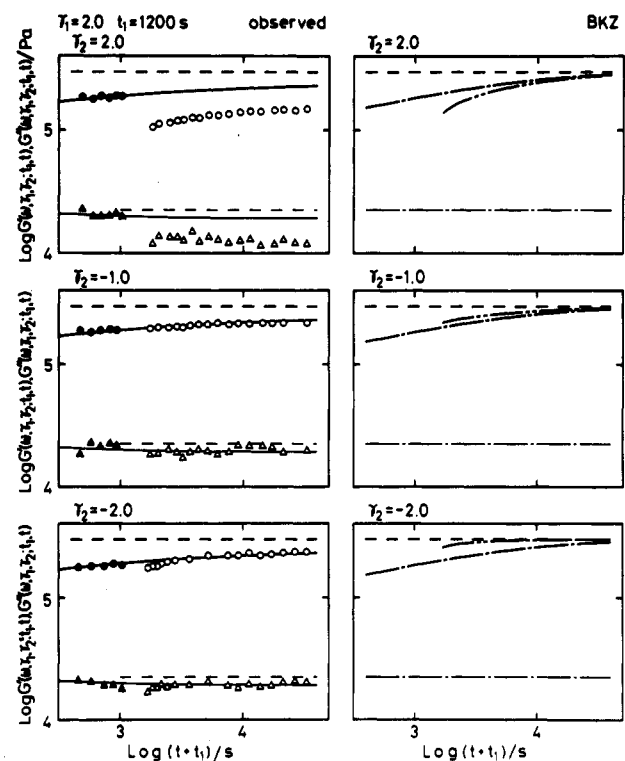


Figure 7. Double-logarithmic plots of $G'(\omega, \gamma_1; t + t_1)$, $G'(\omega, \gamma_1, \gamma_2; t_1, t)$, $G''(\omega, \gamma_1, \gamma_2; t_1, t)$ for various values of γ_2 indicated. $\gamma_1 = 2.0$ and $t_1 = 1200$ s. The meanings of symbols and lines are the same as in Figure 6.

before being strained is shown by a broken line. Our interest is in the behavior of $G'(\omega, \gamma_1, \gamma_2; t_1, t)$. The solid line shows the values predicted by eq 4. The theory predicts that the $G'(\omega, \gamma_1, \gamma_2; t_1, t)$ curve has a maximum when γ_2 is equal to -2 , that is, when the macroscopic deformation of the sample recovers completely. Experimentally, on the other hand, it is evident that

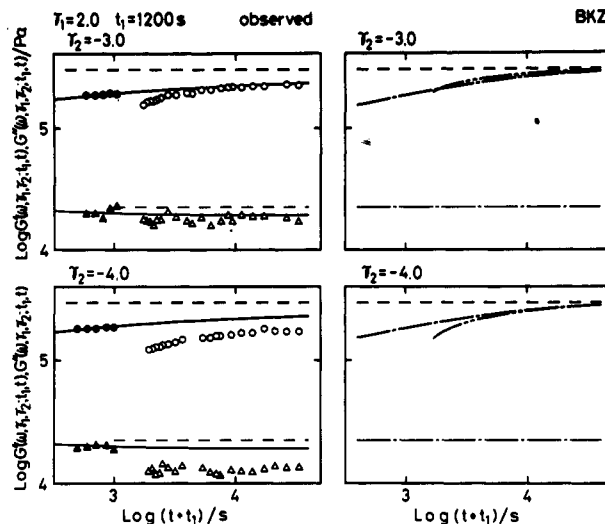


Figure 8. Plots similar to Figure 7 for $\gamma_2 = -3.0$ and -4.0 . $\gamma_1 = 2.0$ and $t_1 = 1200$ s. The meanings of symbols and lines are the same as in Figure 6.

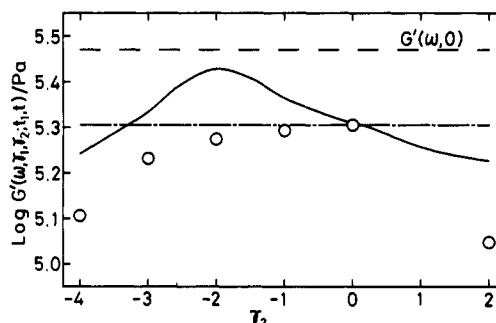


Figure 9. Logarithmic plots of $G'(\omega, \gamma_1, \gamma_2; t_1, t)$ at $t = 1000$ s against γ_2 . $\gamma_1 = 2.0$ and $t_1 = 1200$ s. Circles denote the experimental values. The chain-dashed and the broken lines denote the values of $G'(\omega, \gamma_1; t + t_1)$ and $G'(\omega, 0)$, respectively. The solid line denotes the prediction of the BKZ theory.

$G'(\omega, \gamma_1, \gamma_2; t_1, t)$ never exceeds the chain-dashed line at any value of γ_2 . This means that the entanglement structure never recovers by imposition of any second strain. Combining the results in Figures 6–8 and Figure 9, it may be concluded that the strain externally given to the polymeric materials can destroy the entanglement structure but cannot recover the structure destroyed previously.

Such a discrepancy between the theory and the experiment comes from the implicit postulate of the BKZ theory that not only the configuration of polymer chain but also the entanglement structure would change in the same manner as the macroscopic deformation does. The present experiment may imply that the memory function should be defined corresponding to the structure of the material, as pointed out by Nagasawa et al.^{8–12} Taking into account of a history-dependent structure change in the material, a new phenomenological theory is proposed by Coleman and Zapas.^{13,14} Such a way of thinking may be the fundamental point when we think over a nonlinear constitutive equation.

Acknowledgment. We are greatly indebted to Professor John D. Ferry of the University of Wisconsin and Professor Mitsuru Nagasawa of the Toyota Institute of Technology for their valuable comments.

References and Notes

- Doi, M. *The Theory of Polymer Dynamics*; Clarendon Press: Oxford, 1986.
- Larson, R. G. *Constitutive Equations for Polymer Melts and Solutions*; Butterworth: Boston, 1988.

- (3) Doi, M. *J. Polym. Sci., Polym. Phys. Ed.* **1980**, *18*, 1005.
- (4) Isono, Y.; Itoh, K.; Komiyatani, T.; Fujimoto, T. *Macromolecules*, preceding paper in this issue.
- (5) Bernstein, B.; Kearsley, E. A.; Zapas, L. J. *Trans. Soc. Rheol.* **1963**, *7*, 391.
- (6) Doi, M. *J. Polym. Sci., Polym. Phys. Ed.* **1980**, *18*, 1891.
- (7) Osaki, K.; Kimura, S.; Kurata, M. *J. Rheol.* **1981**, *25*, 549.
- (8) Sakai, M.; Kajiura, H.; Nagasawa, M. *Trans. Soc. Rheol.* **1974**, *18*, 323.
- (9) Kajiura, H.; Sakai, M.; Nagasawa, M. *Trans. Soc. Rheol.* **1976**, *20*, 575.
- (10) Isono, Y.; Nagasawa, M. *Macromolecules* **1980**, *13*, 862.
- (11) Takahashi, Y.; Isono, Y.; Noda, I.; Nagasawa, M. *Macromolecules* **1986**, *19*, 1217.
- (12) Takahashi, Y.; Isono, Y.; Noda, I.; Nagasawa, M. *Macromolecules* **1987**, *20*, 153.
- (13) Coleman, B. D.; Zapas, L. J. *J. Rheol.* **1989**, *33*, 501.
- (14) Zapas, L. J.; Crissman, J. M. *J. Rheol.* **1990**, *34*, 1.